Investigation of the Multi-Threshold Decoding Efficiency in Wireless Communication Systems

Nurlan Tashatov
Research Institute of Information Security and Cryptology, L.N. Gumilyov Eurasian National University, Kazakhstan
tashatov_nn@enu.kz

Gennady Ovechkin
Abylkas Saginov Karaganda Technical University, Kazakhstan
ovechkingv@yahoo.com

Zhuldyz Sailaukyzy
Abylkas Saginov Karaganda Technical University, Kazakhstan
zhuldyzsailaukyzy@gmail.com (corresponding author)

Eldor Egamberdiyev
Research Institute of Information Security and Cryptology, L.N. Gumilyov Eurasian National University, Kazakhstan
eeldoru@gmail.com

Dina Satybaldina
Research Institute of Information Security and Cryptology, L.N. Gumilyov Eurasian National University, Kazakhstan
satybaldina_dzh@enu.kz

Gulmira Danenova
Abylkas Saginov Karaganda Technical University, Kazakhstan
danenovagulmira@gmail.com

Zarina Khassenova
D. Serikbayev East Kazakhstan Technical University, Kazakhstan
zkhasenova@edu.ektu.kz

Received: 22 October 2025 | Revised: 9 November 2025 | Accepted: 19 November 2025

 DOI: https://doi.org/10.48084/etasr.15712

ABSTRACT

Reliable data transmission in 5G and Internet of Things (IoT) systems is limited by multipath fading and Intersymbol Interference (ISI), requiring efficient Forward Error Correction (FEC) with low computational complexity. This paper investigates Multi-Threshold Decoders (MTDs) for Self-Orthogonal Codes (SOCs) in Orthogonal Frequency-Division Multiplexing (OFDM) and Multiple-Input Multiple-Output (MIMO) systems with Space-Time Coding (STC) under International Telecommunication Union – Radio Communication Sector (ITU-R) (Outdoor A, TU6, RA6) and 3GPP Spatial Channel Model (SCM) (Urban Macro/Micro) channels. Using OFDM with 512/1024 subcarriers, SOCs decoded by MTDs were compared with turbo and Low-Density Parity-Check (LDPC) codes (WiMAX 2016; DVB-S2 16/200 and 64/800). The results show that MTDs achieve the same Bit Error Rate (BER) as DVB-S2 LDPC while requiring approximately 30–50 times fewer operations for the same code parameters. In deep fades, MTDs provide up to 1.5 dB BER gain over turbo and WiMAX LDPC codes, with mobility up to 50 km/h having negligible impact. A min-sum refinement provides an additional 1–1.5 dB improvement, and antenna

diversity yields a 4–7 dB Signal-to-Noise Ratio (SNR) gain at BER = 10^{-5}. Open Computing Language (OpenCL)-based GPU acceleration increases throughput from 15 Mbit/s (CPU) to 480 Mbit/s (32× speed-up), confirming scalability for software-defined 5G systems. The proposed MTD framework combines high reliability with low complexity, representing a practical and energy-efficient FEC solution for next-generation 5G and IoT systems.

Keywords-error correction; GPU acceleration; fading channels; Multiple-Input Multiple-Output (MIMO); Multi-Threshold Decoder (MTD); Orthogonal Frequency-Division Multiplexing (OFDM); Open Computing Language (OpenCL); Self-Orthogonal Codes (SOCs); Space-Time Coding (STC)

I. INTRODUCTION

Wireless communication systems are constantly evolving to meet the needs of society and industry for fast, high-quality transmission of large amounts of data with minimal latency and seamless connectivity for billions of devices [1]. Designers must take into account Intersymbol Interference (ISI) and fading, which arise due to the nature of wireless channels [2, 3].

ISI occurs due to reflections from buildings or terrain along which radio waves propagate. Delays in different signal paths result in significant signal overlap, which leads to symbol distortion and a rising Bit Error Rate (BER). To maintain the required BER, it is necessary to accept a decreased data rate, thus decreasing channel capacity.

Fading can be defined as the variation of channel power over time and frequency. It leads to both constructive and destructive interference from the various possible propagation paths between the transmitter and receiver antennas. It occurs on a spatial scale comparable in magnitude to the carrier wavelength and is frequency dependent (small-scale fading). Another type of fading, which is not frequency-dependent, is actually caused by signal attenuation with distance and shadowing by large objects such as buildings and hills. Such large-scale fading is usually taken into account in base station placement plans. Variations in signal amplitude, connection breaks, and degradation of multimedia data transmission quality are caused by small-scale multipath fading. It is aggravated in 5G networks because of the high data rates and density of mobile devices supported, the use of millimeter-wave frequencies, spatial diversity, and multiplexing [4]. When a moving Unmanned Aerial Vehicle (UAV) connects to a ground station, radio waves bounce off the ground and other objects, causing the channel to change quickly and the Doppler shift to occur [5]. Due to the fact that Internet of Things (IoT) devices have very small antennas with limited power, they are more vulnerable to experiencing fading, especially in crowded urban or industrial areas where ISI is more likely to happen [6]. In wireless sensor networks, fading and ISI make data collection difficult because the sensors are low-power and in hard-to-reach places (like forests, underground, or inside buildings). Therefore, several types of wireless communication standards face important design challenges related to channel fading, ISI, and interference suppression.

A variety of techniques are employed in modern wireless communications to enhance signal quality and reduce fading. Among these methods are Orthogonal Frequency-Division Multiplexing (OFDM) [7, 8] combined with diversity techniques and beamforming, spatial diversity techniques, and Multiple-Input Multiple-Output (MIMO) systems [9, 10]. Forward Error Correction (FEC) algorithms are crucial in this context, as they can rectify data compromised by noise, interference, and fading without requiring retransmission [11, 12]. IEEE 802.16m (WiMAX) [13] and EN 302 307 (DVB-S2) [14] standards employ Low-Density Parity-Check (LDPC) codes with varying code lengths and coding rates. These codes, as well as turbo codes, convolutional codes, and polar codes, are required for battery-powered devices in wireless sensor networks, as they provide a balance between computational complexity and error correction efficiency [15]. In 5G mobile networks, polar codes [16] are used for control channels, for which reliability and low latency are important requirements [17, 18]. These codes are not easy to decode, but researchers are developing more effective algorithms [19].

For 6G and future communication systems, in addition to further optimization of polar and LDPC codes, researchers propose exploring machine learning for adaptive coding, optimization of code parameters, and improvement of decoding algorithms, especially in dynamic and complex channels [20]. Another promising direction is the development of new code constructions and decoding algorithms that provide low latency, high performance, low computational complexity, hardware implementation optimization and flexibility, and compatibility with other methods of reducing fading and interference, such as OFDM and MIMO [21, 22].

In this paper, we investigate the performance of iterative decoders for Self-Orthogonal Codes (SOCs) based on the Massey threshold decoder [23], referred to as Multi-Threshold Decoders (MTDs) [24, 25] or Multi-Stage Threshold Decoders [26, 27], for wireless networks. Previous studies of the performance of MTDs in MIMO systems with fading radio channels [28] showed that MTDs could nearly optimally decode even very long codes with low computational complexity, providing high efficiency in such channels.

The application of MTDs for SOCs in MIMO-OFDM wireless channels with multipath effects was examined, approaches to improve their performance in such environments were explored, and aspects of their software implementation using parallel computing technologies were analyzed, allowing the evaluation of their potential for 5G/Beyond and IoT applications.

Although LDPC and turbo codes are widely used in modern wireless standards, their iterative decoding requires high computational resources, which limits their use in low-power and real-time systems such as IoT networks. In contrast, MTDs for SOCs achieve comparable reliability with significantly lower decoding complexity due to simple integer operations and threshold-based logic. This gap motivates our study to

evaluate how MTDs can provide efficient FEC for broadband OFDM/MIMO communication systems where both high reliability and low computational cost are required.

The novelty of this work lies in the software optimization and performance evaluation of MTDs for SOCs in realistic MIMO-OFDM fading channels using Open Computing Language (OpenCL), demonstrating LDPC-level reliability with significantly lower computational complexity.

The following items represent our contributions:

- A complete review of the performance of MTDs for SOCs in MIMO-OFDM systems under several multipath fading channel models (International Telecommunication Union – Radio Communication Sector (ITU-R), Spatial Channel Model (SCM)) was presented, showing the same performance as turbo and LDPC codes but with lower implementation complexity.
- The performance of MTDs in combination with Space-Time Coding (STC) was analyzed, and the optimal transmit and receive antenna configurations, STC matrices, and modulation techniques to increase data transmission reliability were determined.
- For the parallel implementation of multi-threshold decoding of SOCs, a practical application on OpenCL was proposed, providing a speedup of 150× and 12× over CPU and Compute Unified Device Architecture (CUDA) methods, respectively.

II. RELATED WORKS

The outcomes of the review of relevant research on improving error correction and modulation techniques to address issues such as ISI and erasures in MIMO-OFDM wireless communication systems with a focus on 5G and IoT applications are detailed.

Information transmitted over communication channels can be modified by noise and interference, resulting in the data received at the receiver side not matching the data at the transmitter side. To assess the reliability of data transmission, the performance of communication channels is determined by the parameters Signal-to-Noise Ratio (SNR) and BER, or Block Error Rate (BLER) [29]. The higher the SNR, the higher the communication quality and the fewer the errors. The lower the BER, the better the quality of data transmission. Thus, the correlation between BER and SNR is inversely proportional and nonlinear. Channel coding does not change the physical SNR level of the channel. However, it significantly improves the efficiency of using this SNR. Due to its error correction capability, a channel-coded system can achieve the same BER as a system without coding, but under conditions of much lower SNR. ISI and fading do not reduce SNR. They are additional sources of distortion that lead to an increase in BER even at high SNR. FEC schemes encode data by adding redundant bits before transmission. At the receiving side, error correction is performed by reconstructing the corrupted data based on channel code decoding algorithms. Coding methods do not change SNR, but they significantly improve the relationship between BER and SNR. They allow achieving much lower BER at the same SNR level, which makes communication more reliable and efficient.

Channel codes have been developed to an advanced level to ensure the fidelity of modern wireless communication systems. The evolution of FEC techniques aligns with the evolution of mobile communication systems: from simple convolutional codes in 2G to more robust turbo codes in 3G/4G, and finally special classes of LDPC and polar codes used in 5G. The primary task is the discovery and fine-tuning of solutions applicable to massive MIMO and OFDM systems, focusing on fast and efficient software and hardware implementations of encoders and decoders capable of meeting the required performance levels.

Turbo codes, LDPC, and polar codes were simulated under MATLAB by authors in [30] to assess performance under ISI The study modeled a channel using Binary Phase Shift Keying (BPSK) and Additive White Gaussian Noise (AWGN). Two types of equalizers at the receiver front end were used by the researchers to mitigate the adverse effects of ISI: the Zero-Forcing (ZF) equalizer and the Minimum Mean-Square Error (MMSE) equalizer. Simulation results indicated that iterative Least-Squares (LS) estimation of the channel impulse response improved the performance of all three codes, including LDPC codes, polar codes, and turbo codes, within the operational SNR range. The LDPC codes proved to be the most effective in correcting errors over channels suffering from ISI.

Authors in [31] investigated MIMO-OFDM systems with LDPC for Underwater Acoustic Communication (UWA) systems. UWA channels face multipath propagation conditions [32] due to reflections from the water surface, seabed, and obstacles, which reduce link quality. To mitigate ISI, the authors incorporated OFDM, Single Carrier Frequency Domain Equalization (SC-FDE), and a MIMO system with LDPC codes similar to those used in 5G communication systems [33]. Simulation results for a UWA communication with 4×32 MIMO showed performance improvement with LDPC codes on the order of 5 dB. The experiments demonstrated a significant data transmission rate of up to 125.7 kbit/s, as well as spectral efficiency of up to 3.5 bps/Hz.

Authors in [34] proposed an Error Correction Hybrid Coding Algorithm (EC-HCA) combining Quasi-Cyclic LDPC (QC-LDPC) and Space-Time Block Coding (STBC) for MIMO-OFDM systems. This approach mitigates ISI by leveraging STBC to avoid interference among transmit antennas, achieving a Peak Signal-to-Noise Ratio (PSNR) of 10.24 dB in a 2×2 MIMO setup, outperforming methods like Alamouti encoding [35], polar-convolutional coding [36], and optimal power allocation with turbo codes [37].

To satisfy bandwidth constraints and performance requirements, wireless communication engineers and researchers adopt parallel computation technologies. Along with hardware platforms (GPUs, Field-Programmable Gate Arrays (FPGAs), systems-on-chips), the choice of the Application Programming Interface (API), such as CUDA or OpenCL, is critical for developing high-performance encoders and decoders [38].

Authors in [39] describe an LDPC decoder that can run as fast as 10 Gbit/s on a GPU (GeForce RTX 2080Ti). The performance of the (8448, 26, 112) LDPC decoder was tested under an AWGN channel with BPSK modulation. The software implementation of this decoder was written in C using CUDA. The Single Instruction, Multiple Data (SIMD) instructions multiplied by four the number of processed codewords and further parallelized codeword execution. The Early Termination (ET) mechanism reduced the number of decoding iterations at high SNR, almost doubling channel throughput while maintaining the same error correction performance [40-42].

The initial validation of FEC decoders prior to hardware implementation and integration with communication systems has consistently been challenging. A hardware–software methodology utilizing the Xilinx Alveo U200 device and its parallel execution in OpenCL was detailed in [43]. The results demonstrate significant acceleration in both the Hardware Description Language (HDL) modeling and FPGA prototyping.

This study investigates the performance of MTDs for SOCs in MIMO-OFDM wireless channels with multipath fading and ISI. Similar to traditional threshold decoders, MTDs rely on short-integer addition, i.e., checksumming. Thus, their performance limitations are determined only by the maximum data flow rate that shift registers within the decoder can sustain and by how many parallel registers are being employed in the decoding process. Single-bit modulo-2 adders, small-integer adders, and standard shift registers are among the fastest components in current digital hardware. Using this approach for implementing MTDs results in performance levels approximately three orders of magnitude higher than other algorithms under conditions of high noise. An MTD built on an Altera FPGA with 40 decoding iterations yielded about 1.6 Gbit/s throughput [44]. In [45], a CUDA-based decoder reached about 350 Mbit/s on the NVIDIA GTX970 and 815 Mbit/s on the NVIDIA GTX1080 for a code with a block length of 1600 symbols.

In summary, the literature shows active development of coding techniques to combat ISI and fading in modern wireless communication systems. From simple convolutional codes to more complex turbo and LDPC codes, researchers continually enhance algorithmic efficiency. Although LDPC codes perform well over ISI channels, their hardware implementation complexity requires powerful computing platforms (GPUs, FPGAs) and special APIs (CUDA, OpenCL). It is on this note that MTDs have been considered an adequate solution. Due to their low computational complexity based on simple integer operations, MTDs have enormous prospects for parallel implementations and attaining startling performances (on the order of Gbit/s) on FPGAs. They become the code of preference for channels with large ISI and fading, where decoding must be efficient with low hardware implementation costs.

III. BACKGROUND

This section provides an overview of the encoding and decoding algorithms for SOCs based on the principles of threshold decoding. These algorithms are designed to achieve reliable error correction with minimal computational complexity, which is essential for modern high-speed wireless communication systems such as MIMO-OFDM and 5G/IoT networks.

SOCs represent a specialized subclass of convolutional codes that exploit orthogonality conditions to simplify the implementation of threshold-based decoding while maintaining high correction capability. The orthogonality property allows for a reduction in the number of parity-check relationships and simplifies iterative decision-making during the decoding process. Such characteristics make SOCs particularly attractive for systems that require real-time performance and limited hardware resources.

The detailed mathematical background and encoder structures of SOCs were previously reported in our earlier work [46], where the design methodology and parity-check matrix construction were described in detail. The theoretical foundations and algorithmic structures of both threshold and multi-threshold decoding for SOCs were discussed comprehensively in [47], emphasizing their error-correction potential and scalability for different code lengths.

In this study, the focus is placed on the software implementation aspects of these algorithms and on evaluating their performance in MIMO-OFDM wireless channels using GPU acceleration. The described framework establishes a foundation for analyzing and comparing various FEC techniques in subsequent sections.

IV. MATERIALS AND METHODS

This section presents the materials and methods used in the study, including the simulation environment, channel models, modulation schemes, and implementation details necessary to evaluate the performance of the proposed MTD-based FEC approach.

A. Space-Time Coding in Multiple-Input Multiple-Output Systems

The paper studies the efficiency of using MTDs in communication channels with fading when using OFDM technology to combat multipath. When using one transmitting and one receiving antenna, this approach is not efficient enough, since the presence of deep and long fading within one code block usually leads to many errors even after decoding. To improve the reliability of data transmission, it is possible to additionally use spatial diversity during transmission and reception, i.e., to transmit and receive data using several antennas (MIMO systems). In this case, the antennas should be spaced far enough apart that the correlation of signals on them is minimal. Then the probability that all radio signals between all antennas will simultaneously be subject to fading is quite small. As a result, the quality of communication is significantly improved with significantly lower energy costs. It should be noted that when using MIMO technology, there is a supplementary avenue to realize STC. In this case, there are options for increasing the transmission rate (for example, when one antenna transmits one symbol, known as spatial multiplexing) or improving the energy efficiency of

transmission (the signal transmitted by the antenna is a function of several transmitted symbols). This is determined by the space-time code matrix.

Currently, there are many proven STC matrices, including those specified by standards. For example, the IEEE 802.16e (WiMAX) standard specifies 1, 2, 3, and 4 transmit-antenna configurations [48].

When using one transmitting antenna, STC is not used. For two transmitting antennas with STC, the following transmitting matrices can be used:

- Orthogonal Alamouti matrix, code rate 1:

$$A = \begin{bmatrix} S_i & -S'_{i+1} \\ S_{i+1} & S'_i \end{bmatrix} \quad (1)$$

- Non-orthogonal V_BLAST matrix, code rate 2:

$$B = \begin{bmatrix} S_i \\ S_{i+1} \end{bmatrix} \quad (2)$$

- Non-orthogonal matrix, code rate 2:

$$C = \frac{1}{\sqrt{1+r^2}} \begin{bmatrix} S_i + jrS_{i+3} & rS_{i+1} + S_{i+2} \\ S_{i+1} - rS_{i+2} & jrS_i + S_{i+3} \end{bmatrix},\ r = \frac{-1+\sqrt{5}}{2} \quad (3)$$

Here, S_i is the transmitted symbol of the signal constellation, j is the imaginary unit, and S'_i denotes the complex conjugate of S_i.

For four transmit antennas with STC, the following transmitting matrices can be used:

- Orthogonal, code rate 1:

$$A = \begin{bmatrix} S_i & -S'_{i+1} & 0 & 0 \\ S_{i+1} & S'_i & 0 & 0 \\ 0 & 0 & S_{i+2} & -S'_{i+3} \\ 0 & 0 & S_{i+3} & S'_{i+2} \end{bmatrix} \quad (4)$$

- Non-orthogonal, code rate 2:

$$B = \begin{bmatrix} S_i & -S'_{i+1} & S_{i+4} & -S'_{i+5} \\ S_{i+1} & S'_i & S_{i+5} & S'_{i+4} \\ S_{i+2} & -S'_{i+3} & S_{i+6} & -S'_{i+7} \\ S_{i+3} & S'_{i+2} & S_{i+7} & S'_{i+6} \end{bmatrix} \quad (5)$$

- Non-orthogonal, code rate 4:

$$C = \begin{bmatrix} S_i \\ S_{i+1} \\ S_{i+2} \\ S_{i+3} \end{bmatrix} \quad (6)$$

To decode the STC code, a system of equations is first constructed:

$$B = GS + N \quad (7)$$

where S is a column vector of transmitted signals, G is a matrix depending on the channel coefficients, N is complex Gaussian noise, and B is a column vector formed from the received signals. From this expression, using a maximum likelihood detector, an array of logarithms of the likelihood ratio for the bits of each transmitted symbol is obtained.

As an example, let us consider how the matrix G and the vectors S and B are formed for two transmitting antennas using the STC matrix A:

$$S = \begin{bmatrix} S_1 \\ S_2 \end{bmatrix} \quad (8)$$

where S_1 and S_2 are signals transmitted over two time intervals.

$$B = \begin{bmatrix} R_1^{(1)} \\ R_1^{(2)'} \\ \vdots \\ R_n^{(1)} \\ R_n^{(2)'} \end{bmatrix} \quad (9)$$

where $R_k^{(m)}$ is the signal received by the k-th antenna at time m.

$$G = \begin{bmatrix} h_{11}^{(1)} & h_{21}^{(1)} \\ h_{21}^{(2)'} & -h_{11}^{(2)'} \\ \vdots & \vdots \\ h_{1n}^{(1)} & h_{2n}^{(1)} \\ h_{2n}^{(2)'} & -h_{1n}^{(2)'} \end{bmatrix} \quad (10)$$

where $h_{kp}^{(m)}$ is the channel coefficient from the k-th transmitting to the p-th receiving antenna in the m-th time interval.

Three demodulation algorithms were evaluated:

- MMSE demodulation:

$$\hat{\Theta} = (G'G + 2\sigma_n^2 I)^{-1} G'S \quad (11)$$

where I is the identity matrix and σ_n^2 is the noise variance.

- Maximum-Likelihood (ML) demodulation:

$$\hat{\Theta} = \frac{\sum_{\Theta} \Theta \cdot \exp\left\{-\frac{1}{2}(S-G\Theta)'(U)^{-1}(S-G\Theta)\right\}}{\sum_{\Theta} exp\left\{-\frac{1}{2}(S-G\Theta)'(U)^{-1}(S-G\Theta)\right\}} \quad (12)$$

where Θ is the constellation set.

- Approximate ML demodulation, which considers only the constellation point closest to the received signal for soft-decision computation.

Soft decisions from these algorithms are fed to the MTD for error correction, enhancing decoding performance in fading channels.

B. Simulation Details

Standardized wideband fading channel models were adopted to emulate urban, suburban, and rural deployments. The ITU-R channels [49] included Outdoor Channel A, Typical Urban 6 (TU6), and Rural Area 6 (RA6). TU6 was modeled with the delay–power profile [0, 0.2, 0.5, 1.6, 2.3, 5] μs and [–3, 0, –2, –6, –8, –10] dB, respectively. RA6 used equally spaced taps with delays [0, 0.1, 0.2, 0.3, 0.4, 0.5] μs and powers [0, –4, –8, –12, –16, –20] dB. To obtain the spatial

structure essential for MIMO, the 3GPP SCM in Urban Macro (UMa) and Urban Micro (UMi) configurations was utilized, incorporating angle-of-arrival/angle-of-departure spreads and realistic base-station/User Equipment (UE) heights [50, 51]. Doppler frequencies for speeds up to 50 km/h were used for mobility. These models were selected for their compatibility with WiMAX and 5G urban deployments, representing scenarios pertinent to IoT and low-altitude UAV communications characterized by multipath and spatial diversity.

OFDM with two Fast Fourier transform (FFT) sizes (512 and 1,024 subcarriers) was used at the physical layer. To balance spectral efficiency and ISI robustness, Cyclic Prefix (CP) ratios of 1/8 and 1/16 were used in each scenario.

Quadrature Phase-Shift Keying (QPSK), 8 Phase-Shift Keying (8-PSK), 16 Adaptive Phase-Shift Keying (16-APSK), and 16 Quadrature Amplitude Modulation (16-QAM) constellations were considered. For each scenario, the constellation order was chosen to find a balance between spectral efficiency and implementation complexity. In low-SNR or high-diversity setups, QPSK was used as the base; in the same bandwidth, 8-PSK was used when moderate spectral efficiency was needed. 16-APSK and 16-QAM were enabled in higher-throughput settings and combined with stronger channel coding and/or spatial multiplexing as appropriate. In SCM-based MIMO studies, 16-QAM was configured for cases emphasizing spatial multiplexing, whereas 16-APSK was used in the OFDM settings following DVB-S2-compatible mapping.

Antenna configurations (1×1, 2×2, and 4×4) were evaluated. STC employed matrices A, B, and C to cover orthogonal and non-orthogonal designs at different code rates. For two transmit antennas, matrix A provided a rate-1 orthogonal design, whereas matrices B and C provided higher-rate, non-orthogonal options. For four transmit antennas, both rate-1 orthogonal and higher-rate non-orthogonal designs were instantiated. The selection of STC and spatial mode (diversity or multiplexing) depended on the target spectral efficiency and channel model. Receiver processing assumed per-subcarrier channel state information adequate for STC decoding.

Demodulators included MMSE and approximate ML detectors. The detector choice was aligned with the modulation order and MIMO/STC setting to balance complexity and soft-information quality.

Coding options covered SOCs decoded via MTD, LDPC codes [52] from IEEE 802.16e (WiMAX) and DVB-S2, and turbo codes [53]. The code lengths in the study included 2,016 bits (WiMAX LDPC), ~10,000 bits (turbo), 16,200 and 64,800 bits (DVB-S2 LDPC), and SOC lengths around 36,864 and 64,800 bits. LDPC decoding used a normalized or offset min-sum algorithm, whereas turbo decoding used the max-log-MAP algorithm. Table I shows a summary of the most important simulation settings and options.

The simulation environment was built in MATLAB, and C was used to speed up the performance of the encoder, decoder, and other complex processing blocks that required significant computational power. The simulations were carried out on a workstation that met the specifications shown in Table II.

TABLE I. CHANNEL EXPERIMENTAL PARAMETERS

Component	Specification / parameter
Channel	ITU-R: Outdoor A, TU6, RA6 SCM: UMa, UMi
Mobility	0–50 km/h (Doppler per carrier frequency)
OFDM	FFT=512 or 1,024; CP=1/8 or 1/16
MIMO/STC	1×1, 2×2, 4×4; STC matrices A (orthogonal, rate 1), B (non-orthogonal, rate 2), C (non-orthogonal, rate 2 or 4)
Modulation	QPSK, 8-PSK, 16-APSK, 16-QAM
Demodulation	MMSE; approximate ML
Coding	SOC+MTD (36,864 and 64,800 bits; ⩽25 iterations); LDPC (WiMAX 2016 bits; DVB-S2 16,200 bits, 64,800 bits); Turbo (≈10,000 bits)
Decoding	SOC (MTD, ⩽25 iterations); LDPC (min-sum); Turbo (max-log-MAP)
Code rates	SOC R≈1/2; DVB-S2 LDPC R=1/2; Turbo R=1/2

TABLE II. WORKSTATION SPECIFICATIONS

Component	Specification
Processor	Intel Core i7 4790K
Motherboard	ASUS Z97
Graphics card	NVIDIA Quadro K4000
RAM	Kingston 16 GB
HDD	Western Digital RE 4 TB

C. Software Implementation of the Multi-Threshold Decoder for Self-Orthogonal Codes

In addition to the previous implementation of an MTD for SOCs on CUDA, a portable OpenCL implementation targeted at heterogeneous devices, including systems-on-chips and FPGA accelerators, was developed. The primary goal is not to outperform existing CUDA kernels on NVIDIA GPUs, but rather to (i) create an implementation functionally equivalent to the base CUDA version, and (ii) evaluate the performance of the same multi-threshold decoding algorithm for SOCs on non-NVIDIA architectures.

The decoder is written in OpenCL 1.2. The OpenCL kernels implement the same SOC+MTD algorithmic pipeline as our original CUDA implementation. This pipeline includes fixed-point Log-Likelihood Ratio (LLR) thresholding, multi-pass updates, syndrome checks, and early termination logic (Figure 1).

V. RESULTS AND DISCUSSION

This section presents and analyzes the simulation results obtained in this study. It includes a comparative performance evaluation of MTD for SOCs, LDPC codes, and turbo codes under multipath fading conditions. In addition, the section examines the impact of employing STC on system performance, as well as the benefits of GPU acceleration in enhancing decoding speed.

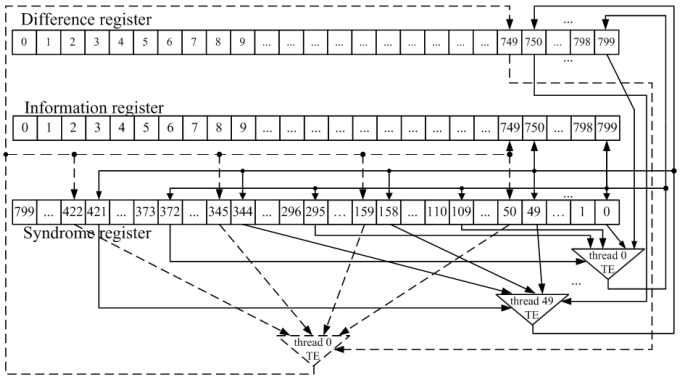

Fig. 1. Multi-threshold decoder using 50 concurrent threads.

A. *Performance of the Multi-Threshold Decoder for Self-Orthogonal Codes and Other Error Correction Methods in Multipath Channels*

This section presents simulation results evaluating the performance of MTDs for SOCs and other error correction methods in standard ITU-R and SCM channel models. For MTD simulations, extensive parameter optimization was performed, including the selection of the code, number of decoding iterations, threshold values, weight coefficients for each iteration, and the method for determining syndrome weights.

Figure 2 illustrates the BER performance of MTDs for a SOC with a code rate of 1/2 and a length of about 32,000 bits as a function of SNR per bit (E_b/N_0) in an Outdoor Channel A environment using different types of modulation (curves labeled "SOC, MTD, ..."). In this case, a demodulator was used that formed only hard decisions regarding the decoded bits (the use of soft decisions from the demodulator will improve the characteristics by another 1–1.5 dB). OFDM with 1,024 subcarriers and main parameters from the IEEE 802.16e (WiMAX) standard was also applied. The guard interval represented one-sixteenth of the total OFDM symbol duration. Note that when using 8-PSK modulation, the energy loss relative to QPSK is about 3 dB, and when using 16-APSK modulation, the loss is about 5 dB. At the same time, these modulation schemes increase the bit rate by 1.5 and 2 times, respectively, without expanding the frequency band.

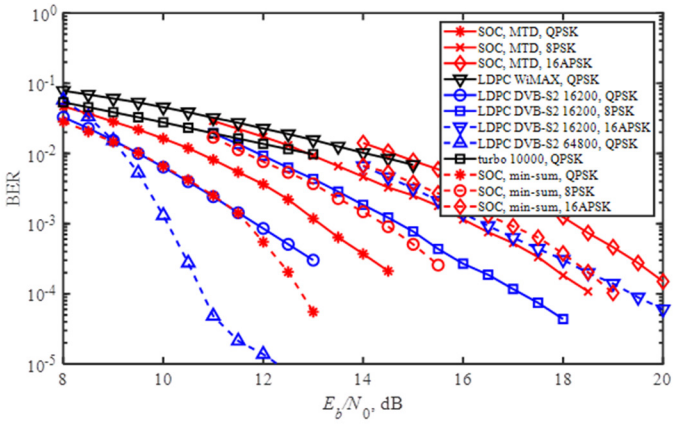

Fig. 2. BER performance in the ITU-R Outdoor Channel A.

A detailed comparison of BER performance and decoding complexity for MTD, LDPC, and turbo codes is summarized in Table III.

TABLE III. COMPARATIVE PERFORMANCE METRICS OF MTD, LDPC, AND TURBO CODES

Code	Length	Rate	BER (12 dB)	Complexity	Observation
MTD (SOC)	36,864	1/2	1.0×10^{-5}	1×	Low-complexity baseline
MTD (min-sum)	36,864	1/2	6.5×10^{-6}	1.2×	+1–1.5 dB vs MTD
LDPC (WiMAX)	2,016	1/2	2.5×10^{-4}	~30×	Weak in deep fades
LDPC (DVB-S2)	16,200	1/2	8.0×10^{-6}	~40×	Similar BER, heavy decoding
Turbo (3GPP)	10,000	1/2	2.0×10^{-4}	~30×	Slow convergence

Figure 2 also shows the "turbo..." curve representing a turbo code with a code rate of 1/2 and a block length of about 10,000 bits using QPSK modulation with the same channel and OFDM parameters. The constructive length of the component codes was equal to 4. The max-log-MAP algorithm was used to decode the component codes. Note that the turbo code characteristics are significantly worse than those of the MTD due to the fact that such a code length is insufficient to cope with fading in the communication channel.

The characteristics of a fairly short LDPC code from the IEEE 802.16e (WiMAX) standard with a length of 2,016 bits, using the same transmission parameters, are also shown in Figure 2 by the "LDPC WiMAX, ..." curve. The min-sum decoding algorithm was used in this case. It should be noted that this code copes with fading as poorly as the turbo code. Longer LDPC codes from the DVB-S2 standard (16,200 and 64,800 bits, code rate 1/2) achieve better BER, as shown by the curves "LDPC DVB-S2 16,200, ..." and "LDPC DVB-S2 64,800, ...". These codes are already capable of providing BER performance slightly better than MTD. However, as already noted, the complexity of implementing these decoders is tens of times greater than that of MTD. Moreover, for SOCs used in conjunction with MTD, with an insignificant increase in complexity (approximately 4 times), it is possible to achieve the characteristics shown in Figure 2 by the curves "SOC, min-sum, ..." for the QPSK, 8-PSK, and 16-APSK modulation types. These results are better than the characteristics of the basic MTD by approximately 1–1.5 dB and comparable to the results provided by the LDPC codes of length 16,200 from the DVB-S2 standard. It should be noted that similar results were obtained for other ITU-R channel models, and the main conclusions were consistent.

Figure 3 illustrates the performance of these codes in the SCM Urban Macro channel model (results were obtained for other SCM types as well). The OFDM modulation parameters are the same as those in Figure 2. The figure shows SOC performance for QPSK and 16-QAM at receiver speeds of 0 and 50 km/h (curves "SOC,..."), as well as turbo codes (~10,000 bits, curve "turbo...") and LDPC codes from the DVB-S2 standard (16,200 bits, curve "LDPC DVB-S2,

16,200...", 64,800 bits, curve "LDPC DVB-S2, 64,800...") and from the IEEE 802.16e (WiMAX) standard (curve "LDPC WiMAX..."). Note that the transmitter and receiver movement at 50 km/h has virtually no effect on the observed performance. Furthermore, the relative efficiency of turbo, short and long LDPC codes compared with the MTD for SOCs remains the same as in the ITU-R channel model.

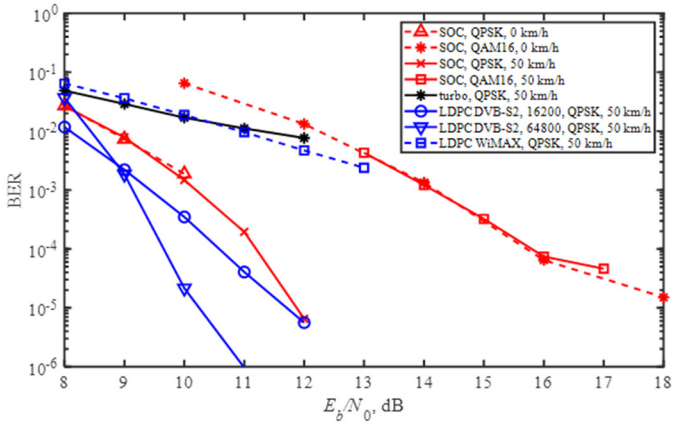

Fig. 3. BER performance in the SCM Urban Macro channel.

B. *Application of Space-Time Coding with Multi-Threshold Decoders in Fading Channels*

The simulation employed a multi-threshold decoder with 25 decoding iterations for the constructed SOC, which had a code rate of R = 8/16, a code distance of 17, and a length of 36,864 bits. OFDM multiplexing with 512 carriers was used in conjunction with MTD, with a guard interval equal to 1/8 of the OFDM symbol length. Conventional QPSK was applied in the simulation. The channel simulation used the default six-path TU6 profile of COST 259 recommendation with a delay profile of [0, 0.2, 0.5, 1.6, 2.3, 5] μs and a power profile of [–3, 0, –2, –6, –8, –10] dB. The maximum Doppler frequency was equal to 0 Hz.

Figure 4 presents the MTD performance using different numbers of transmit and receive antennas (1×1, 2×2, 4×4) with different STC matrices. Note that the energy efficiency increases significantly with an increase in the number of antennas. Furthermore, for two transmit and receive antennas with the same STC rate, matrix C proves to be the best. When operating with four transmit antennas, matrix B, for which the STC code rate is 2, has the best energy efficiency. When switching to matrix C, which allows for the transmission of twice as much data in the same time, the energy efficiency degrades by approximately 2 dB.

Figure 5 shows the MTD performance under the above-described conditions using various demodulation algorithms. Using the approximate optimal algorithm (curves labeled "app opt"), the results are almost 2 dB better than those obtained with the MMSE algorithm. This means that the quality of soft decisions under these conditions greatly influences the effectiveness of the error correction scheme.

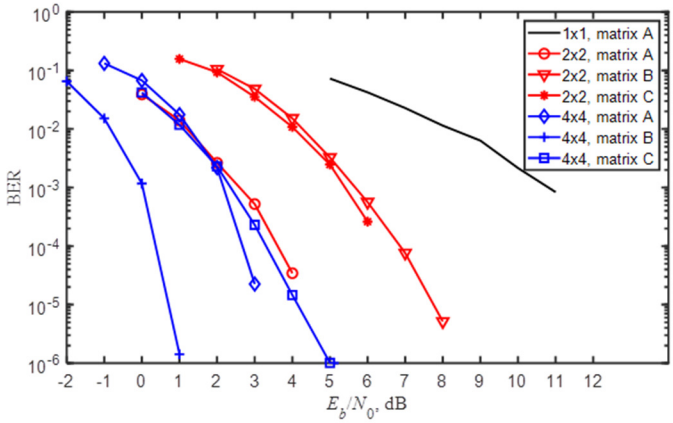

Fig. 4. MTD performance for different STC matrices and antenna configurations.

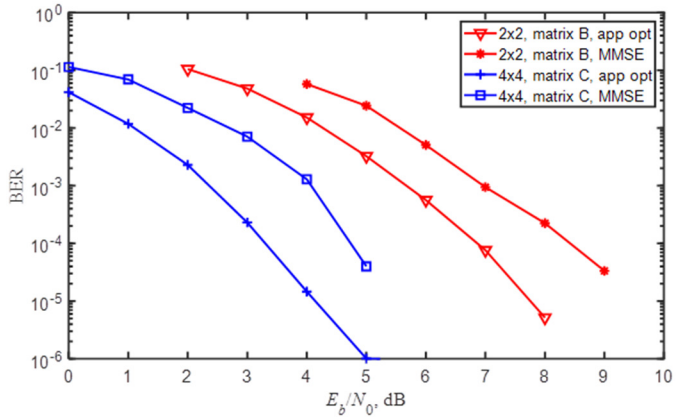

Fig. 5. MTD performance for different demodulation algorithms.

Figure 6 evaluates MTD performance across different channel profiles. In addition to TU6, the six-beam RA6 profile from the same COST 259 recommendation was used. It is characterized by a delay profile of [0, 0.1, 0.2, 0.3, 0.4, 0.5] μs (equidistant beams) and a power profile of [0, -4, -8, -12, -16, -20] dB. The MMSE algorithm was used for demodulation. Note that the reflected beams have lower power than in TU6. As a result, the efficiency of the data transmission system for such a channel is approximately 2 dB worse than for TU6.

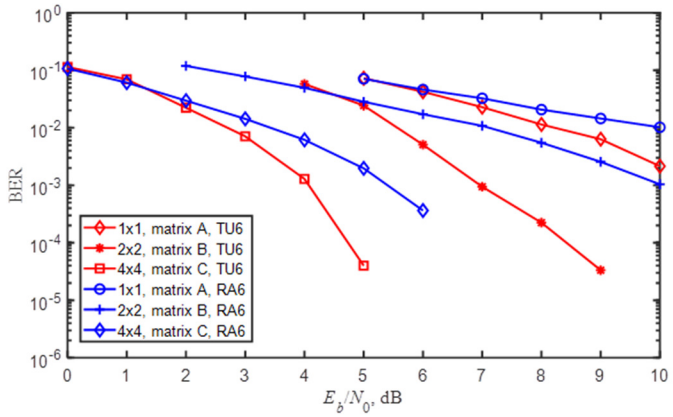

Fig. 6. MTD performance for different channel profiles.

Below are the results comparing the efficiency of the SOC with MTD and LDPC codes for the SCM Urban Micro scenario using MIMO. To combat multipath, OFDM multiplexing with the parameters discussed earlier was again used. The noise-correcting codes were an SOC with a code rate of 1/2 and a length of 32,768 bits, decoded using MTD, and an LDPC code of the DVB-S2 standard with a code rate of 0.44 and a length of 16,200 bits. In Figure 7, the curves "SOC, 1×1, QPSK" and "LDPC, 1×1, QPSK" present the dependences of the decoding error probability of the SOC and the LDPC code on the SNR per bit (E_b/N_0) using QPSK modulation. In this case, a demodulator that generates only hard decisions regarding the decoded bits was used. It should be noted that these codes provide approximately the same data transmission reliability. When switching to two transmit and two receive antennas, the system's energy efficiency decreases slightly (curves "SOC, 2×2, QPSK" and "LDPC, 2×2, QPSK"), but the bit rate doubles without expanding the used bandwidth.

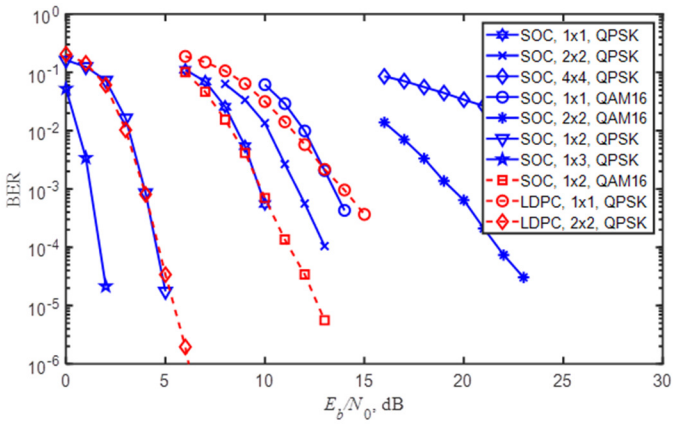

Fig. 7. Simulation results in the SCM Urban Micro channel with MIMO.

Note that for MTD, the same increase in data rate is achieved by switching to 16-QAM modulation instead of QPSK, but the efficiency of such a system (curve "SOC, 1×1, 16-QAM") is almost 2 dB worse than the MIMO variant. It should also be noted that the effect of using MIMO technology for SOCs was greater than for LDPC codes. If the bit rate does not increase (using a single transmit antenna and QPSK modulation), using multiple receive antennas can significantly improve data transmission reliability. An example of the characteristics of such systems for two and three receiving antennas is shown in Figure 7 by the curves "SOC, 1×2, QPSK" and "SOC, 1×3, QPSK". The gain compared to one receiving antenna, at a target decoding error probability per bit of 10^{-5}, was 4 and 7 dB, respectively. The same improvement is obtained when using LDPC codes (curve "LDPC, 1×2, QPSK").

From Figure 7, it also follows that when attempting to further increase the data transmission rate using MIMO, the MTD characteristics deteriorate significantly (curves "SOC, 4×4, QPSK" and "SOC, 2×2, 16-QAM"). Therefore, such options for increasing the transmission rate are impractical to use in practice, or additional methods to improve the characteristics are required.

C. GPU-Accelerated Simulation Performance

A data-parallel scheme [54] was adopted, in which each independent codeword was processed end-to-end by a single OpenCL work-item. All MTD stages, including LLR calculation, threshold tests, bit updates, syndrome checks, and early stopping, were executed sequentially within that work-item, preserving the required ordering without cross-item synchronization. Parallelism was achieved by launching many such items concurrently, one per dataset. This maximizes device occupancy and eliminates global synchronization overhead, whereas local memory buffers are used to stage per-codeword data and tables:

```
kernel decode_mtd(codeword_i):
  // local buffers for the i-th code word
  preload_indices_to_local()
  llr = load_llr_i()
  for iter in 1..I_max:
    apply_thresholds(llr) // sequential
    steps of the MPD algorithm
    update_bits_and_metrics()
    if check_syndrome(): break
  store_decision_i()
```

This approach achieved a simulation throughput of 300 kbit/s (see Table III), which, however, is insufficient. Based on these unsatisfactory results, a study was conducted to identify the bottleneck limiting simulation throughput. This bottleneck turned out to be memory access. This is due to the specific memory architecture in OpenCL, where the data being processed can be stored in local or global memory [55]. Due to architectural features, accessing global memory takes significantly longer than accessing local memory. It was therefore hypothesized that decoder and encoder performance could be improved by minimizing global memory access and maximizing local memory utilization.

To address the identified bottleneck, the data-parallel SOC+MTD scheme was restructured to maximize the use of local memory. Each work-group processed a batch of K codewords: LLRs and index tables were fetched from global memory using coalesced vector loads and staged in double-buffered local memory (A/B). All MTD iterations were then run in-place on local buffers; only final decisions and optional statistics were written back to global memory. Where supported, subgroup collectives (ballot, shuffle, popcount) were used to accelerate thresholding and reductions. This scheme minimizes global-memory traffic, reduces synchronization overhead, and improves device occupancy.

The proposed approach maximized GPU resource utilization, increasing the data transmission system simulation speed on a PC equipped with a NVidia Quadro K4000 GPU to 120 Mbit/s. As Table IV shows, the OpenCL implementation with minimized global memory access achieved an 8-fold increase in throughput over the CPU implementation, although it remained considerably lower than that of the parallel CUDA decoder.

As previously noted, the OpenCL implementation was designed primarily for portability, including deployment on

OpenCL-enabled FPGAs, rather than to achieve the same performance as the CUDA model. OpenCL remained the preferred method when cross-vendor compatibility and FPGA portability were required, providing a unified approach for hardware implementation of channel coding systems.

TABLE IV. DECODING SPEED OF MULTI-THRESHOLD DECODERS FOR SOCS

Ref.	Device (GPU/CPU)	Compute model	Throughput (Mbit/s)
[25]	Intel Core i7-4770 (4 cores)	Baseline (no GPU)	15
[45]	NVIDIA GeForce GTX 970	Standard GPU pipeline: CUDA kernels	350
[45]	Intel Core i7 4770K + NVIDIA GeForce GTX 1080	Standard GPU pipeline: CUDA kernels	815
Proposed	Intel Core i7 4790K + NVIDIA Quadro K4000	OpenCL kernels (data-parallel)	120
Proposed	Intel Core i7 4790K + NVIDIA Quadro K4000	OpenCL kernels (local-memory optimized)	480

VI. CONCLUSION

The paper presents new results on the efficiency of Multi-Threshold Decoders (MTDs) for Self-Orthogonal Codes (SOCs) in multipath fading channels with Intersymbol Interference (ISI), combined with Orthogonal Frequency-Division Multiplexing (OFDM) and Space-Time Coding (STC). Simulation results demonstrate that MTDs achieve nearly the same Bit Error Rate (BER $\approx 1\times10^{-5}$ at $E_b/N_0 = 12$ dB) as DVB-S2 Low-Density Parity-Check (LDPC) codes while requiring approximately 30–50× fewer operations. The min-sum refinement provides an additional 1–1.5 dB gain, and antenna diversity yields a 4–7 dB Signal-to-Noise Ratio (SNR) improvement at BER = 10^{-5}. The OpenCL-based GPU implementation increased decoding throughput from 15 Mbit/s on a CPU to 480 Mbit/s, a 32× speed-up, confirming the scalability of MTDs for high-speed software-defined communication systems.

Further research will focus on Field-Programmable Gate Array (FPGA)-based hardware realization of the MTD architecture and its integration with adaptive modulation, hybrid Forward Error Correction (FEC) schemes, and machine learning-based optimization to reduce latency and power consumption in next-generation 5G/6G and Internet of Things (IoT) networks.

ACKNOWLEDGMENT

The research was funded by the Science Committee of the Ministry of Higher Education and Science of the Republic of Kazakhstan under grant "AP19679505 – Research for multi-threshold decoding of convolutional codes and their software and hardware implementation for high-speed radio channels with fading."

REFERENCES

[1] M. Alsabah *et al.*, "6G Wireless Communications Networks: A Comprehensive Survey," *IEEE Access*, vol. 9, pp. 148191–148243, 2021, https://doi.org/10.1109/ACCESS.2021.3124812.

[2] S. R. Saunders and A. A. Aragón-Zavala, *Antennas and Propagation for Wireless Communication Systems*, 3rd ed. Hoboken, NJ, USA: John Wiley & Sons, 2024, https://doi.org/10.1002/9781119332206.

[3] A. F. Molisch, *Wireless Communications: From Fundamentals to Beyond 5G*, 3rd ed. Hoboken, NJ, USA: John Wiley & Sons, 2022.

[4] A. Darghouthi, A. Khlifi, and B. Chibani, "Performance Analysis of 5G Waveforms over Fading Environments," in *2021 International Wireless Communications and Mobile Computing*, Harbin City, China, 2021, pp. 2182–2187, https://doi.org/10.1109/IWCMC51323.2021.9498589.

[5] J. Viana *et al.*, "Increasing Reliability on UAV Fading Scenarios," *IEEE Access*, vol. 10, pp. 30959–30973, 2022, https://doi.org/10.1109/ACCESS.2022.3149588.

[6] L. Xiao, S. Li, Y. Qian, D. Chen, and T. Jiang, "An Overview of OTFS for Internet of Things: Concepts, Benefits, and Challenges," *IEEE Internet of Things Journal*, vol. 9, no. 10, pp. 7596–7618, May 2022, https://doi.org/10.1109/JIOT.2021.3132606.

[7] A. Sayed, M. Khatun, T. Ahmed, A. A. Piya, P. Chakraborty, and T. Choudhury, "Performance Analysis of OFDM System on Multipath Fading and Inter Symbol Interference (ISI) Using AWGN," in *3rd International Conference on Computational Intelligence in Pattern Recognition*, Kolkata, West Bengal, India, 2022, pp. 25–36, https://doi.org/10.1007/978-981-16-2543-5_3.

[8] A. B. Narasimhamurthy, M. K. Banavar, and C. Tepedelenlioğlu, *OFDM Systems for Wireless Communications*. Cham, Switzerland: Springer International Publishing, 2010, https://doi.org/10.1007/978-3-031-01513-7.

[9] S. A. Janawade, P. Krishnan, K. Kandasamy, S. S. Holla, K. Rao, and A. Chandrasekar, "A Low-Complexity Solution for Optimizing Binary Intelligent Reflecting Surfaces towards Wireless Communication," *Future Internet*, vol. 16, no. 8, Aug. 2024, Art. no. 272, https://doi.org/10.3390/fi16080272.

[10] P. Sharma, R. N. Tiwari, P. Singh, P. Kumar, and B. K. Kanaujia, "MIMO Antennas: Design Approaches, Techniques and Applications," *Sensors*, vol. 22, no. 20, Oct. 2022, Art. no. 7813, https://doi.org/10.3390/s22207813.

[11] R. Kadel, K. Paudel, D. B. Guruge, and S. J. Halder, "Opportunities and Challenges for Error Control Schemes for Wireless Sensor Networks: A Review," *Electronics*, vol. 9, no. 3, Mar. 2020, Art. no. 504, https://doi.org/10.3390/electronics9030504.

[12] M. Bettayeb, S. Ghunaim, N. Mohamed, and Q. Nasir, "Error Correction Codes in Wireless Sensor Networks: A Systematic Literature Review," in *2019 International Conference on Communications, Signal Processing, and their Applications*, Sharjah, United Arab Emirates, 2019, pp. 1–6, https://doi.org/10.1109/ICCSPA.2019.8713725.

[13] *IEEE Standard for Local and Metropolitan Area Networks Part 16: Air Interface for Fixed Broadband Wireless Access Systems*, IEEE Std 802.16-2004 (Revision of IEEE Std 802.16-2001), 2004, https://doi.org/10.1109/IEEESTD.2004.226664.

[14] *Digital Video Broadcasting (DVB); Second generation framing structure, channel coding and modulation systems for Broadcasting, Interactive Services, News Gathering and other broadband satellite applications; Part 1: DVB-S2*, EN 302 307-1-V1.4.1, 2014.

[15] M. M. Ali, S. J. Hashim, M. A. Chaudhary, G. Ferré, F. Z. Rokhani, and Z. Ahmad, "A Reviewing Approach to Analyze the Advancements of Error Detection and Correction Codes in Channel Coding With Emphasis on LPWAN and IoT Systems," *IEEE Access*, vol. 11, pp. 127077–127097, 2023, https://doi.org/10.1109/ACCESS.2023.3331417.

[16] E. Arikan, "A performance comparison of polar codes and Reed-Muller codes," *IEEE Communications Letters*, vol. 12, no. 6, pp. 447–449, June 2008, https://doi.org/10.1109/LCOMM.2008.080017.

[17] K. Arora, J. Singh, and Y. S. Randhawa, "A survey on channel coding techniques for 5G wireless networks," *Telecommunication Systems*, vol. 73, no. 4, pp. 637–663, Apr. 2020, https://doi.org/10.1007/s11235-019-00630-3.

[18] N. Kumar, D. Kedia, and G. Purohit, "A review of channel coding schemes in the 5G standard," *Telecommunication Systems*, vol. 83, no. 4, pp. 423–448, Aug. 2023, https://doi.org/10.1007/s11235-023-01028-y.

[19] C. Zhu, Y. He, and Z. Dou, "Polar Code BP Decoding Optimization for Green 6G Satellite Communication: A Geometry Perspective," *Axioms*, vol. 14, no. 3, Mar. 2025, Art. no. 174, https://doi.org/10.3390/axioms14030174.

[20] C. Shivappa, N. K. Ramaswamy, R. C. Mullegowda, R. K. Ramaswamy, and M. Srikantaswamy, "Efficient Low-Complexity Encoding and Decoding Algorithms for Global Navigation Satellite Systems," *Engineering, Technology & Applied Science Research*, vol. 15, no. 4, pp. 25499–25506, Aug. 2025, https://doi.org/10.48084/etasr.11457.

[21] A. Elsanousi and S. Oztürk, "Performance Analysis of OFDM and OFDM-MIMO Systems under Fading Channels," *Engineering, Technology & Applied Science Research*, vol. 8, no. 4, pp. 3249–3254, Aug. 2018, https://doi.org/10.48084/etasr.2209.

[22] M. Rowshan, M. Qiu, Y. Xie, X. Gu, and J. Yuan, "Channel Coding Toward 6G: Technical Overview and Outlook," *IEEE Open Journal of the Communications Society*, vol. 5, pp. 2585–2685, 2024, https://doi.org/10.1109/OJCOMS.2024.3390000.

[23] J. L. Massey, "Threshold decoding," Ph.D. dissertation, Dept. of Electrical Engineering, Massachusetts Institute of Technology, Cambridge, MA, USA, 1963.

[24] V. V. Zolotarev and G. V. Ovechkin, "Algorithm of multithreshold decoding for Gaussian channels," *Automation and Remote Control*, vol. 69, no. 6, pp. 1086–1100, June 2008, https://doi.org/10.1134/S0005117908060180.

[25] V. V. Zolotarev, Y. B. Zubarev, and G. V. Ovechkin, *Optimization Coding Theory and Multithreshold Algorithms*. Geneva, Switzerland: International Telecommunication Union, 2015.

[26] M. Ahsan Ullah, K. Okada, and H. Ogiwara, "Multi-Stage Threshold Decoding for Self-Orthogonal Convolutional Codes," *IEICE Transactions on Fundamentals of Electronics, Communications and Computer Sciences*, vol. E93.A, no. 11, pp. 1932–1941, 2010, https://doi.org/10.1587/transfun.E93.A.1932.

[27] M. A. Ullah, R. Omura, T. Sato, and H. Ogiwara, "Multi-Stage Threshold Decoding of High Rate Convolutional Codes for Optical Communications," in *AICT 2011, The Seventh Advanced International Conference on Telecommunications*, St. Maarten, The Netherlands Antilles, 2011, pp. 87–93.

[28] G. Ovechkin, D. Satybaldina, Z. Sailaukyzy, G. Danenova, and N. Tashatov, "Methods of Multi-Threshold Decoders Use in Mimo Systems And Methods of Assessing Their Performance," in *2024 8th International Symposium on Innovative Approaches in Smart Technologies*, Istanbul, Turkey, 2024, pp. 1–6, https://doi.org/10.1109/ISAS64331.2024.10845577.

[29] M. Yang, C. Bian, and H.-S. Kim, "OFDM-Guided Deep Joint Source Channel Coding for Wireless Multipath Fading Channels," *IEEE Transactions on Cognitive Communications and Networking*, vol. 8, no. 2, pp. 584–599, June 2022, https://doi.org/10.1109/TCCN.2022.3151935.

[30] A.-M. Cuc, F. L. Morgoș, and C. Grava, "Performance Analysis of Turbo Codes, LDPC Codes, and Polar Codes over an AWGN Channel in the Presence of Inter Symbol Interference," *Sensors*, vol. 23, no. 4, Feb. 2023, Art. no. 1942, https://doi.org/10.3390/s23041942.

[31] M. Marques da Silva, R. Dinis, J. Aleixo, and L. M. L. Oliveira, "On the Performance of LDPC-Coded MIMO Schemes for Underwater Communications Using 5G-like Processing," *Applied Sciences*, vol. 12, no. 11, June 2022, Art. no. 5549, https://doi.org/10.3390/app12115549.

[32] M. Stojanovic and J. Preisig, "Underwater acoustic communication channels: Propagation models and statistical characterization," *IEEE Communications Magazine*, vol. 47, no. 1, pp. 84–89, Jan. 2009, https://doi.org/10.1109/MCOM.2009.4752682.

[33] M. Marques da Silva, R. Dinis, and G. Martins, "On the Performance of LDPC-Coded Massive MIMO Schemes with Power-Ordered NOMA Techniques," *Applied Sciences*, vol. 11, no. 18, Sept. 2021, Art. no. 8684, https://doi.org/10.3390/app11188684.

[34] V. G. Tikka and R. Sivashanmugam, "Error Correction Using Hybrid Coding Algorithm for BER Reduction in MIMO-OFDM," *International Journal of Intelligent Engineering and Systems*, vol. 15, no. 6, pp. 618–626, Dec. 2022, https://doi.org/10.22266/ijies2022.1231.55.

[35] S. Ghazi-Maghrebi and B. Akbarian, "Improved Performance of Alamouti Scheme Using Cyclic Delay Diversity and Doppler Diversity for MIMO Systems-Based," *Wireless Personal Communications*, vol. 116, no. 3, pp. 1971–1992, Feb. 2021, https://doi.org/10.1007/s11277-020-07775-4.

[36] A. Agarwal and S. N. Mehta, "PC-CC: An advancement in forward error correction using polar and convolutional codes for MIMO-OFDM system," *Journal of King Saud University - Computer and Information Sciences*, vol. 32, no. 8, pp. 917–927, Oct. 2020, https://doi.org/10.1016/j.jksuci.2017.12.003.

[37] S. Pyla, P. R. K, and B. S. N, "Capacity and BER performance improvement in integrated MIMO-OFDM system using optimal power allocation, channel estimation, and turbo coding," *International Journal of Communication Systems*, vol. 34, no. 14, Sept. 2021, Art. no. e4915, https://doi.org/10.1002/dac.4915.

[38] A. Asaduzzaman, A. Trent, S. Osborne, C. Aldershof, and F. N. Sibai, "Impact of CUDA and OpenCL on Parallel and Distributed Computing," in *2021 8th International Conference on Electrical and Electronics Engineering*, Antalya, Turkey, 2021, pp. 238–242, https://doi.org/10.1109/ICEEE52452.2021.9415927.

[39] J. Dai, H. Yin, Y. Lv, W. Xu, and Z. Yang, "Multi-Gbps LDPC Decoder on GPU Devices," *Electronics*, vol. 11, no. 21, Nov. 2022, Art. no. 3447, https://doi.org/10.3390/electronics11213447.

[40] R. Li, X. Zhou, H. Pan, H. Su, and Y. Dou, "A High-Throughput LDPC Decoder Based on GPUs for 5G New Radio," in *2020 IEEE Symposium on Computers and Communications*, Rennes, France, 2020, pp. 1–7, https://doi.org/10.1109/ISCC50000.2020.9219558.

[41] C. Tarver, M. Tonnemacher, H. Chen, J. Zhang, and J. R. Cavallaro, "GPU-Based, LDPC Decoding for 5G and Beyond," *IEEE Open Journal of Circuits and Systems*, vol. 2, pp. 278–290, 2021, https://doi.org/10.1109/OJCAS.2020.3042448.

[42] J. Ling and P. Cautereels, "Fast LDPC GPU Decoder for Cloud RAN," *IEEE Embedded Systems Letters*, vol. 13, no. 4, pp. 170–173, Dec. 2021, https://doi.org/10.1109/LES.2021.3052714.

[43] D. Suárez, V. Fernández, H. Posadas, and P. Sánchez, "Accelerating the Verification of Forward Error Correction Decoders by PCIe FPGA Cards," *IEEE Embedded Systems Letters*, vol. 15, no. 3, pp. 157–160, Sept. 2023, https://doi.org/10.1109/LES.2022.3218289.

[44] V. Zolotarev, G. Ovechkin, A. Issainova, D. Satybaldina, and N. Tashatov, "Effective multithreshold decoding algorithms for wireless communication channels," in *2016 IEEE 10th International Conference on Application of Information and Communication Technologies*, Baku, Azerbaijan, 2016, pp. 1–5, https://doi.org/10.1109/ICAICT.2016.7991760.

[45] V. Zolotarev, G. Ovechkin, P. Ovechkin, D. Satybaldina, N. Tashatov, and D. Sankibayev, "High Throughput Software Multithreshold Decoder on GPU," in *2016 Third International Conference on Mathematics and Computers in Sciences and in Industry*, Chania, Greece, 2016, pp. 168–171, https://doi.org/10.1109/MCSI.2016.039.

[46] V. Zolotarev, G. Ovechkin, D. Satybaldina, N. Tashatov, A. Adamova, and V. Mishin, "Efficiency multithreshold decoders for self- orthogonal block codes for optical channels," *International Journal of Circuits, Systems and Signal Processing*, vol. 8, pp. 487–495, 2014.

[47] L. Bouyukliev, S. Bouyuklieva, T. A. Gulliver, and P. R. J. Ostergard, "Classification of Optimal Binary Self-Orthogonal Codes," *Journal of Combinatorial Mathematics and Combinatorial Computing*, vol. 59, pp. 33–87, Jan. 2006.

[48] *IEEE Standard for Local and Metropolitan Area Networks - Part 16: Air Interface for Fixed and Mobile Broadband Wireless Access Systems - Amendment for Physical and Medium Access Control Layers for Combined Fixed and Mobile Operation in Licensed Bands*, IEEE Std 802.16e-2005 and IEEE Std 802.16-2004/Cor 1-2005 (Amendment and Corrigendum to IEEE Std 802.16-2004), Feb. 2006, https://doi.org/10.1109/IEEESTD.2006.99107.

[49] *Guidelines for evaluation of radio transmission technologies for IMT-2000*, Recommendation ITU-R M.1225, 1997.

[50] "Spatial channel model for Multiple Input Multiple Output (MIMO) simulations (Release 6)," 3rd Generation Partnership Project (3GPP), Sophia Antipolis, France, Technical report 3GPP TR 25.996 V6.1.0, 2003.

[51] "Study on 3D channel model for LTE (Release 12)," 3rd Generation Partnership Project (3GPP), Sophia Antipolis, France, Technical report 3GPP TR 36.873, 2014.

[52] D. J. C. MacKay and R. M. Neal, "Near Shannon limit performance of low density parity check codes," *Electronics Letters*, vol. 32, no. 18, pp. 1645–1646, Aug. 1996, https://doi.org/10.1049/el:19961141.

[53] C. Berrou, A. Glavieux, and P. Thitimajshima, "Near Shannon limit error-correcting coding and decoding: Turbo-codes. 1," in *Proceedings of ICC '93 - IEEE International Conference on Communications*, Geneva, Switzerland, 1993, pp. 1064–1070 vol.2, https://doi.org/10.1109/ICC.1993.397441.

[54] H. Xiao, B. Guo, H. Zhang, and C. Li, "A Parallel Algorithm of Image Mean Filtering Based on OpenCL," *IEEE Access*, vol. 9, pp. 65001–65016, 2021, https://doi.org/10.1109/ACCESS.2021.3068772.

[55] Khronos Group, *The OpenCL™ Specification*, Version 3.0. Beaverton, OR, USA: Khronos Group, 2021.